Supplementary Data for "INTERSTITIAL FLOW ENHANCES FORMATION, CONNECTIVITY, AND FUNCTION OF 3D BRAIN MICROVASCULAR NETWORKS GENERATED WITHIN MICROFLUIDIC DEVICE" by Winkelman *et al*., 2021

Supplementary Methods

S.1 Calculation of fibrin hydrogel permeability

The permeability of the fibrin gel (4 mg/mL) was calculated by measuring the velocity of the dextran solution across the hydrogel channel of MFDs from AIM Biotech (Singapore) at multiple hydrostatic pressures (0.375, 0.75, 1.125, and 1.5 mmH_2O). The dextran solution velocity (v) was determined by measuring the distance traveled by the dextran solution front between two time points. The dextran solution volumetric flow rate (Q) was calculated using the following equation:

$$Q = v \times A \tag{S1}$$

where A is the average cross-sectional area of the hydrogel channel. For all differential pressure values, the same 4 experimental replicates were used to measure average dextran solution velocity values. After each round of imaging, the hydrogel channel was washed three times with PBS for 5 minutes at 37°C to remove any remaining dextran solution in the fibrin hydrogel.

The average dextran solution volumetric flow rate measured at 0.375, 0.75, 1.125, and 1.5 mmH_2O were used to determine the fibrin hydrogel permeability (K) using Darcy's Law:

$$K = \frac{Q\mu L}{AP} \tag{S2}$$

where μ is the viscosity of EGM-2 at 37°C (7.5×10^{-3} dyn·s/cm^2)(1), L is the length of the hydrogel channel, and P is the pressure difference across the fibrin hydrogel. The volumetric flow rate measured at 0 mmH_2O was not used because the movement of the dextran solution was dependent solely on diffusion. The four calculated fibrin hydrogel permeabilities were then averaged and used in the following equations, derived by Sudo and colleagues(2), to model interstitial flow velocity, $v(t)$, and the volumetric flow rate, $Q(t)$, at a given time, t, across the fibrin hydrogel:

$$v(t) = \frac{\rho g K \Delta h_0}{\mu L} e^{-\frac{\rho g A K}{\mu A_R L} t} \tag{S3}$$

$$Q(t) = \frac{\rho g A K \Delta h_0}{\mu L} e^{-\frac{\rho g A K}{\mu A_R L} t} \tag{S4}$$

where ρ is the density of EGM-2 (assumed to be 1000 kg/m^3), g is gravitational acceleration, Δh_0 is the volume height difference between high-pressure and low-pressure reservoirs at $t = 0$, and A_R is the cross-sectional area of the reservoirs. Interstitial flow velocity and volumetric flow rates were plotted using Prism (GraphPad Software).

S.2 Calculation of microsphere velocity and microvessel shear stress

A hydrostatic pressure difference of 0.75 mmH_2O was created to promote the flow of microspheres through MVNs developed under both static and flow conditions. In ImageJ, time lapse images were used to approximate the velocity of microspheres as they flowed through microvessels. Microspheres were selected under the criteria that they were mobile and located near the center of the microvessel. Stationary microspheres were not selected due to the possibility that they were adhered to the microvessel wall. The distance traveled (l) by a microsphere between two time points (t_1, t_2) was used to calculate the microsphere velocity (v_{max}) using the following equation:

$$v_{max} = \frac{l}{(t_2 - t_1)} \tag{S4}$$

This velocity was assumed to be the maximum velocity of the culture medium in the microvessel. At the midpoint of the distance traveled by a microsphere, the radius of the microvessel (r) was measured. Assuming the lumen of the microvessels were circular, the volumetric flow rate (Q) was calculated using the following equation:

$$Q = \frac{v_{max}}{2} \times (\pi r^2) \tag{S5}$$

With the volumetric flow rate, the shear stress (τ) experienced by the microvessel was then calculated using the following equation:

$$\tau = \frac{4\mu Q}{\pi r^3} \tag{S6}$$

where μ is viscosity of the EGM-2 at 37°C(1). To generate average microsphere velocity and microvessel shear stress values, twenty microspheres were analyzed from one sample cultured under static and flow culture.

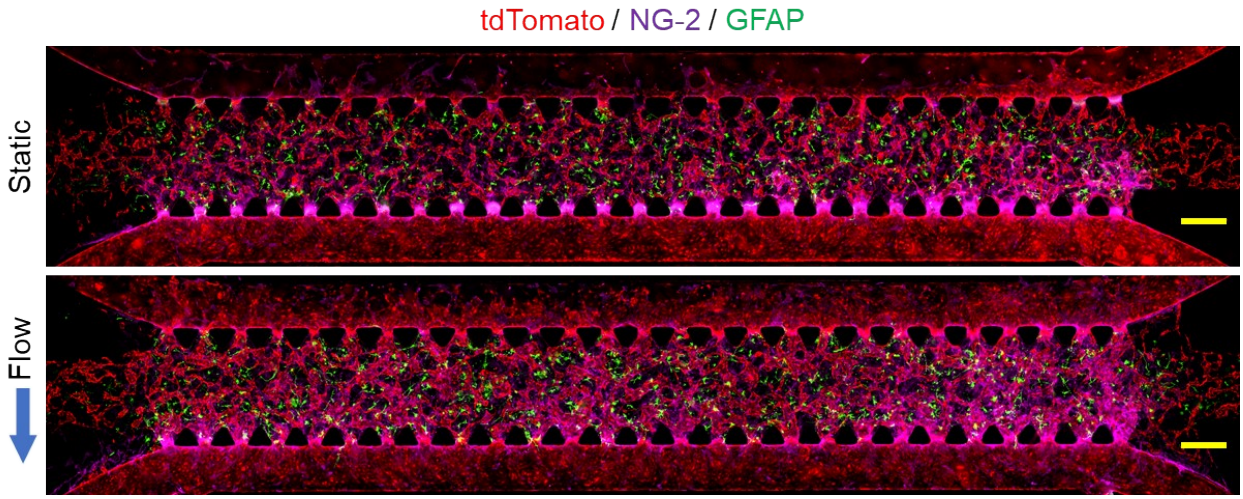

Supplementary Figure 1. Immunocytochemistry of brain MVNs in MFDs. Fluorescence images show maximum intensity projections of brain MVNs cultured under static and flow conditions in MFDs (AIM Biotech) for 8 days. BECs (tdTomato, red) formed microvessels supported by PCs (NG-2, purple) and ACs (GFAP, green) in both conditions. Images show the entire length of the hydrogel and fluidic channels of MFDs. No evidence of significant fibrin gel degradation was observed. Blue arrow indicates direction of interstitial flow induced during flow condition. Scale bars indicate 500 μm.

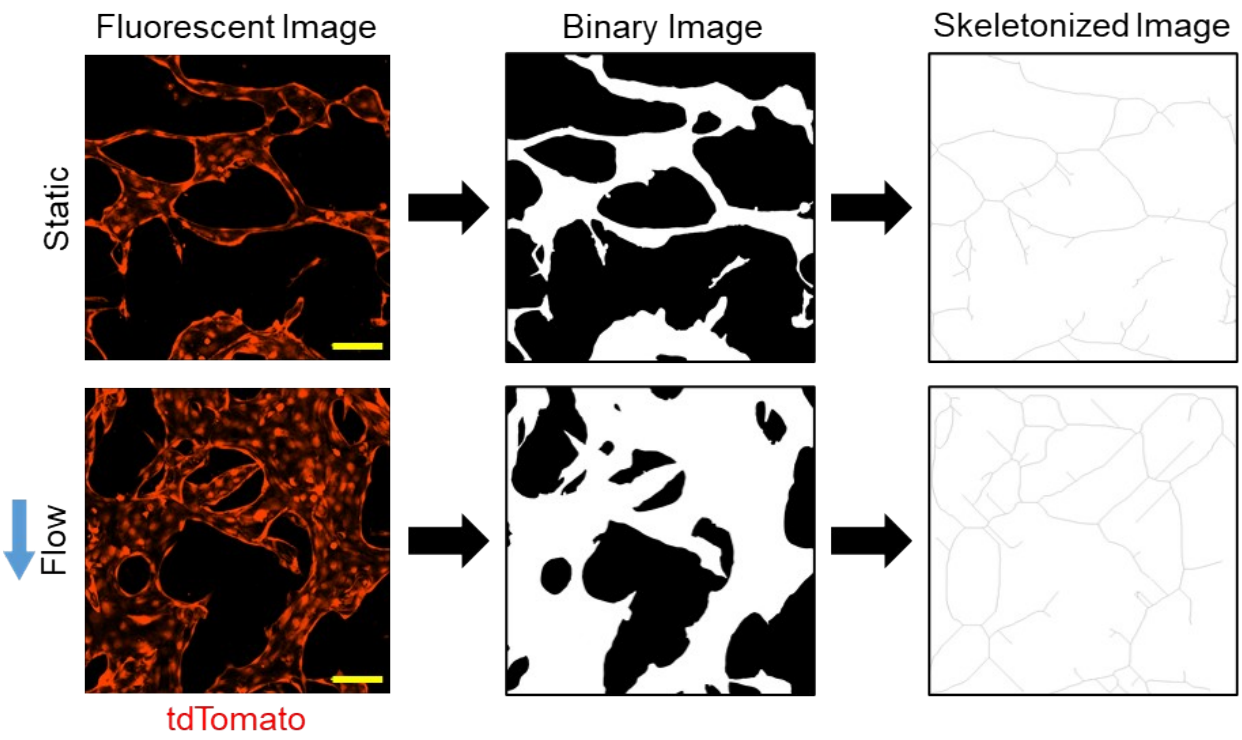

Supplementary Figure 2. Schematic of the image processing pipeline used to quantify microvessel morphology. Inputs were maximum intensity projections of fluorescence confocal images of microvessels (tdTomato, red) from static and flow culture. Blue arrow indicates direction of interstitial flow. Scale bars indicate 100 μm. Next, the fluorescence images were made binary to determine total vessel area. Then, binary images were skeletonized using ImageJ plugin, Skeletonize. Finally, Analyze Skeleton (2D/3D), was used to determine branch number, average branch length, average branch diameter, and the number of blood vessel segments.

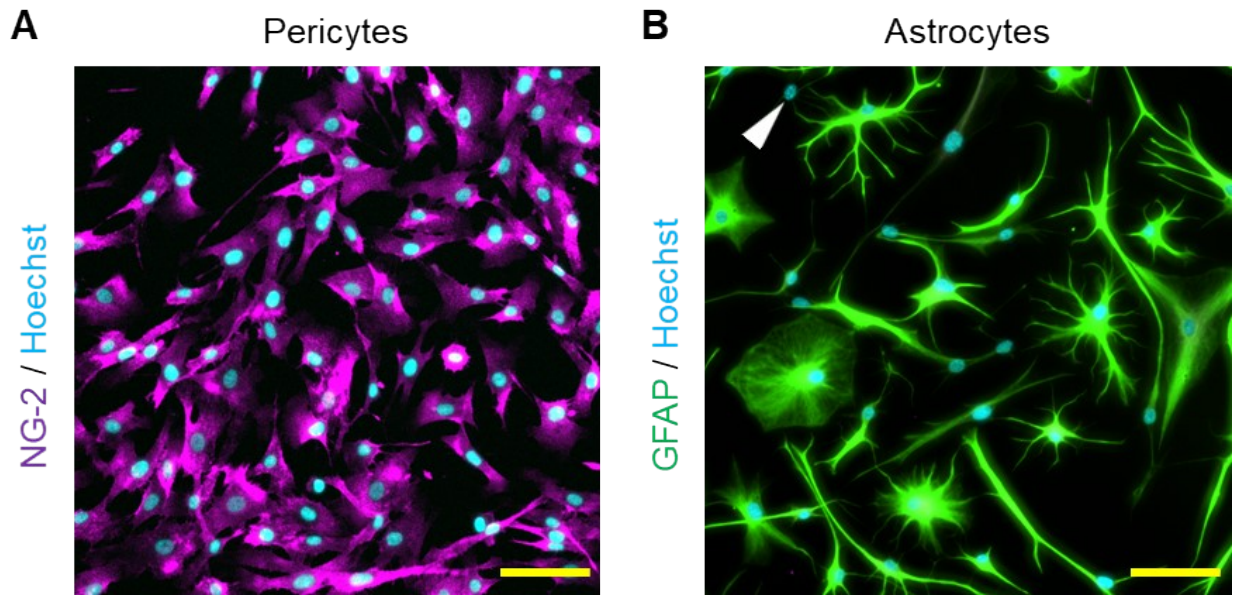

Supplementary Figure 3. PC and AC immunocytochemistry. A, B) Fluorescence images of ScienCell PCs (A) and ACs (B) after 3 days of 2D cell culture. Nuclei were identified with Hoechst (blue). Scale bars indicate 100 µm. A) All PCs visibly express NG-2 (purple). B) Most ACs visibly express GFAP (green). White triangle identifies nucleus with no visible GFAP signal.

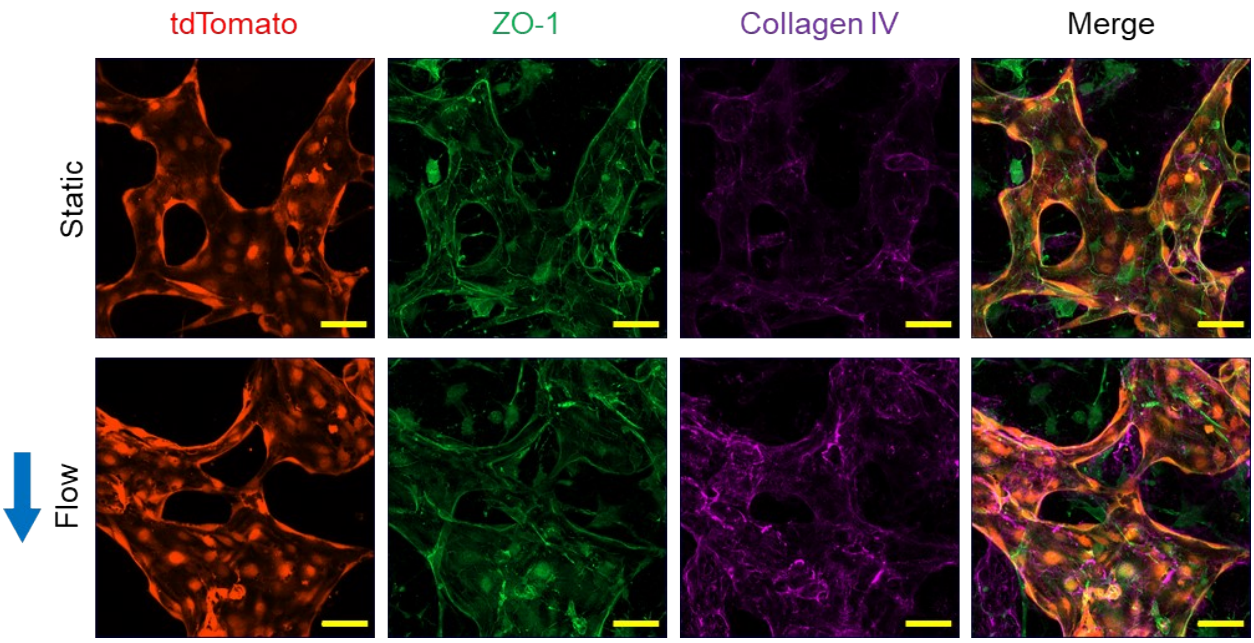

Supplementary Figure 4. Immunocytochemistry of BEC proteins. Maximum intensity projections of fluorescence confocal images of microvessels (tdTomato, red) cultured under static and flow conditions simultaneously stained for ZO-1 (green) and collagen IV (purple). No significant difference was found for the mean ZO-1 fluorescence intensity between static and flow samples. The mean collagen IV fluorescence intensity was found to be higher in flow samples. Quantitative analysis shown in Fig. 7D. Blue arrow indicates direction of interstitial flow. Scale bars indicate 50 μm.

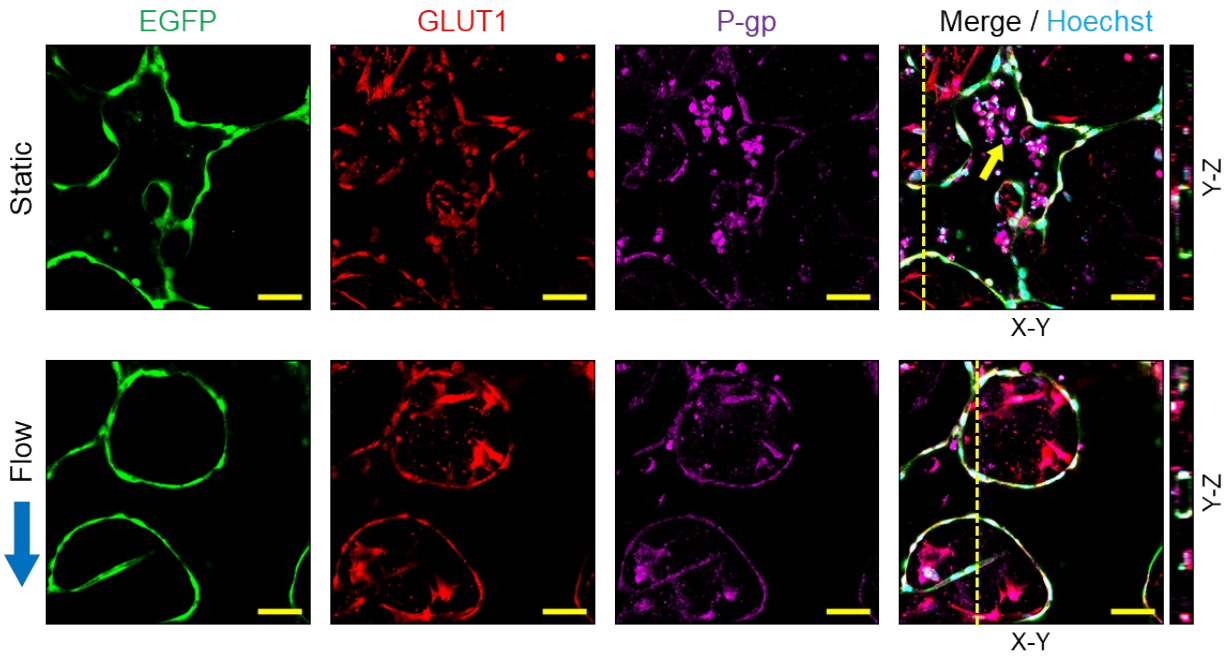

Supplementary Figure 5. Immunocytochemistry of brain MVN proteins. Fluorescence confocal images of brain MVNs cultured under static and flow conditions for 8 days. Brain MVN samples are labeled for GLUT1 (red) and P-gp (purple). Nuclei are labeled with Hoechst (blue). Merge images show X-Y plane and the cross-section of the Y-Z plane at the yellow dashed line. Blue arrow indicates direction of interstitial flow. Yellow arrow identifies a cluster of what are assumed to be dead cells with fragmented nuclei in the lumen of microvessels cultured under static conditions. Scale bars indicate 50 μm. BECs (EGFP, green) express both GLUT1 and P-gp at the border of microvessel lumen in both static and flow conditions. Cells in the interstitial space that express GLUT1 and P-gp, but not EGFP, are either PCs or ACs.

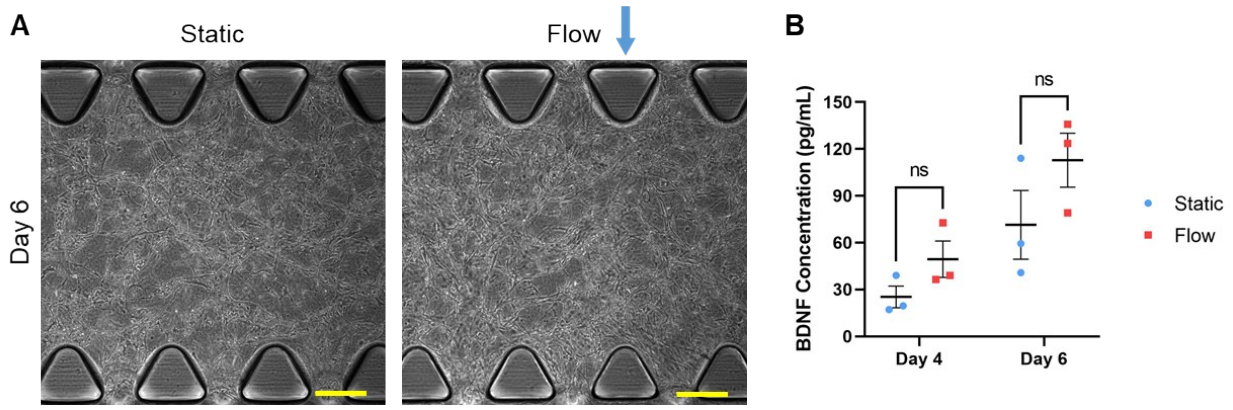

Supplementary Figure 6. Enzyme-linked immunosorbent assay (ELISA) of BDNF. A) Phase images of MVNs cultured under static and flow conditions containing BECs, PCs, and ACs on Day 6. Scale bars indicate 200 µm. Blue arrow indicates direction of interstitial flow. B) Graph of the BDNF concentration detected in culture medium conditioned by MVNs in static and flow cultures on Day 4 and Day 6. Conditioned medium for ELISA was collected every 48 hours. The volume heights of reservoirs containing conditioned medium were reestablished every 24 hours. In flow conditions, interstitial flow rate became negligible approximately 9 hours after volume reestablishment. It was assumed that diffusion would equilibrate the concentration of soluble BDNF throughout MFD fluidic channels in the remaining 15 hours before conditioned medium collection. The data show mean value, error bars ± SEM, n = 3, ns $p > 0.05$.

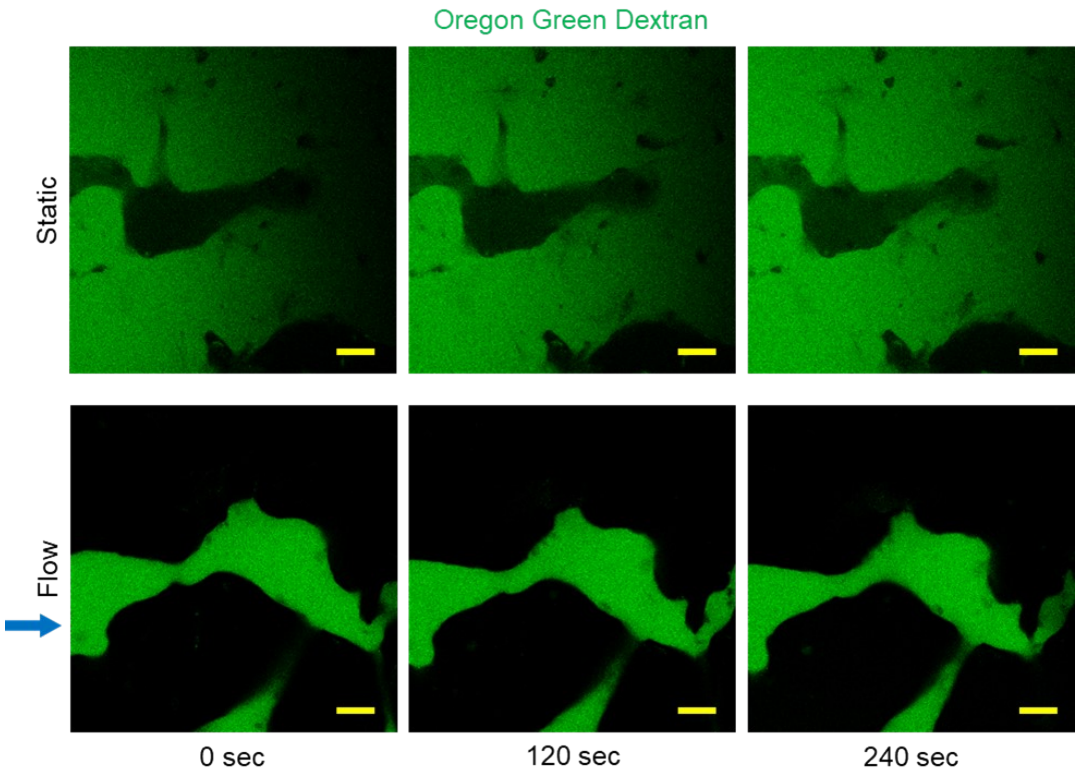

Supplementary Figure 7. Preliminary dextran perfusion assay. Fluorescence time-lapse confocal images of microvessels (not shown) cultured under static and flow conditions perfused with Oregon Green 70 kDa dextran (green) at 0, 120, and 240 seconds. Images were acquired after dextran was allowed to significantly diffuse into the hydrogel channel. In static conditions, microvessels in the center of the hydrogel channel were non-perfused. The borders of microvessels became visible as the dextran solution flowed through the fibrin gel. In flow conditions, dextran solution was perfused through the open lumen of microvessels. Blue arrow indicates direction of interstitial flow. Scale bars indicate 50 μm.

Supplementary Table 1. Primary Antibodies for Immunocytochemistry					
Target Species	**Target Protein**	**Host Species**	**Company**	**Catalog Number**	**Concentration**
Human	NG-2	Mouse	eBioscience	14-6504-80	1:100
Human	GFAP	Rabbit	Invitrogen	PA1-10019	1:1000
Human	ZO-1	Rabbit	Invitrogen	40-2200	1:100
Human	Collagen IV	Mouse	Abcam	ab86042	1:100
Human	Laminin	Rabbit	Abcam	ab11575	1:100
Human	GLUT1	Rabbit	Abcam	ab115730	1:100
Human	P-gp	Mouse	Sigma	P7965	1:50

Supplementary Table 2. Secondary Antibodies for Immunocytochemistry					
Host Species	**Target Species**	**Excitation Wavelength**	**Company**	**Catalog Number**	**Concentration**
Goat	Rabbit	488	Invitrogen	A11034	1:500
Goat	Rabbit	647	Invitrogen	A32733	1:500
Goat	Mouse	594	Invitrogen	A32742	1:500
Goat	Mouse	647	Invitrogen	A21236	1:500

Supplementary Video 1. Fluorescence time-lapse video of microspheres (green) flowing through microvessels (tdTomato, red) formed under static conditions at a hydrostatic pressure of 0.75 mmH_2O. Maximum intensity projection shown in Fig. 4B.

Supplementary Video 2. Fluorescence time-lapse video of microspheres (green) flowing through microvessels (tdTomato, red) formed under flow conditions at a hydrostatic pressure of 0.75 mmH_2O. Maximum intensity projection shown in Fig. 4B.

Supplementary References

1. dela Paz NG, Walshe TE, Leach LL, Saint-Geniez M, D'Amore PA. Role of shear-stress-induced VEGF expression in endothelial cell survival. J Cell Sci [Internet]. 2012 Feb 15 [cited 2021 Jan 20];125(4):831–43. Available from: https://jcs.biologists.org/content/125/4/831
2. Sudo R, Chung S, Zervantonakis IK, Vickerman V, Toshimitsu Y, Griffith LG, et al. Transport-mediated angiogenesis in 3D epithelial coculture. FASEB J [Internet]. 2009 Jul [cited 2021 Feb 26];23(7):2155–64. Available from: /pmc/articles/PMC2718841/